PULL-IN INSTABILITY OF NANO-SWITCHES BASED ON HYBRID NONLOCAL EULER-BERNOULLI BEAM MODEL

N. Taghavi, H. Nahvi*

Mechanical Engineering Department, Isfahan University of Technology, Imam Khomeini Ave. Isfahan, Iran, P.O.Box:

**hnahvi@cc.iut.ac.ir*

Keywords: Nano-switch, Hybrid nonlocal beam model, Eringen's nonlocal beam model, Pull-in voltage.

Abstract

In this article, pull-in instability of cantilever and fixed-fixed nano-switches subjected to electrostatic forces that produced by an applied voltage, and intermolecular forces are investigated. The effect of small length-scale is taken into account, using hybrid nonlocal Euler-Bernoulli beam model. The effects of small length-scale on the pull-in instability and freestanding behavior of the cantilever and fixed-fixed nano-beams are presented and compared with the Eringen's nonlocal, and classical beam models. It is found that Eringen's nonlocal beam model produces unreasonable pull-in voltages, minimum gaps and detachment lengths and the shortcomings of the Eringen's nonlocal beam theory can be resolved by the use of hybrid nonlocal beam model.

1 Introduction

In recent years, NEMS (Nanoelectromechanical systems) and their applications are gaining great interest among researchers. Nano-switches are important building blocks in NEMS. Typically, a nano-switch contains fixed and deformable structures (electrodes), separated by a dielectric medium. When a voltage is applied between the deformable and fixed structures, due to the induced charges, electrostatic forces act on both structures. Since the fixed structure cannot move, the movable structure tends to approach to the fixed one and elastic force tends to take the movable structure back into the undeformed position. Exceeding the applied voltage above a certain value makes the movable electrode to collapse onto the fixed structure. This voltage value is denoted as the pull-in voltage [1].

With the decrease in dimensions, many essential phenomena appear at the nanoscales which are not important at macro scales. In this paper, two effects are investigated in the simulation of pull-in instability of the beam-type nano-switches. The first issue that appears at the nanoscale is the effect of intermolecular forces. In the nanometer range, with the decrease of dimension of the gap between the two electrodes of a nano-switch, the intermolecular forces such as van der Waals and Casimir forces become important. The second effect that appears at the nanoscale is the size dependency of the material characteristics. From theoretical point of view, the classical continuum mechanics is not suitable for interpreting the size-dependent behaviors of nano structures; therefore, the non-classical continuum theories such as nonlocal

elasticity [2] are proposed to explain the size-dependent behaviors of nano structures. In order to account the small-scale effect, Yang et al. [3] investigated the pull-in instability of nano-switches subjected to the electrostatic force produced by the applied voltage and intermolecular force (van der Waals and Casimir forces) within the framework of nonlocal elasticity theory. They proposed a linear distributed load (LDL) model to obtain closed-form solutions for cantilever and fixed-fixed nano-switches. They found that in cantilever nano-switches, an increase in the small-scale factor leads to a higher pull-in voltage, whereas in fixed–fixed nano-switches, it leads to a lower pull-in voltage.

Although, the theory of nonlocal elasticity has been widely used when considering the small-scale effect in nanotechnology, a paradoxical conclusion arises in some cases. In order to resolve this paradox, Challamel and Wang [4] proposed the hybrid nonlocal Euler-Bernoulli beam model.

This paper introduces a new formulation for the pull-in stability of nano-switches under electrostatic and intermolecular forces. By employing the hybrid nonlocal Euler-Bernoulli beam model, the governing equations of the beam-like movable electrodes of the cantilever and fixed-fixed nano-switches are derived and closed-form solutions are presented based on the LDL model. Finally, the effects of the small length-scale on the pull-in voltages, detachment lengths and minimum electrode/ground gaps of the nano-switches are examined.

2 Hybrid nonlocal Euler-Bernoulli beam model

Figure 1(a) and 1(b) show two typical nano-switches with two parallel conducting electrodes, one fixed and the other movable. In Figure 1(a), the movable electrode is modeled as a cantilever nano-beam and in Figure 1(b), it is modeled as a fixed-fixed nano-beam. In both cases, the nano-beams have a uniform cross-section with a width of w and a thickness of h. The electrodes are separated by the dielectric spacer with an initial gap of g. The lengths of the cantilever and fixed-fixed nano-beams are L and $2L$, respectively. As shown in Figure 1(d), for the fixed-fixed beam, both the geometry and simulated lateral load are symmetric about the mid-point of the beam. Hence, the deflection and stress distributions are symmetric as well, and thus, only the left half of the beam with the length of L is considered in the analysis. In both cases, due to the electrostatic and intermolecular forces, the beams deflect towards the fixed electrode. At a critical "pull-in" voltage, beams become unstable and collapse or pull-in onto the fixed electrode. The voltage and deflection of the switches at this state are called pull-in voltage and pull-in deflection, respectively.

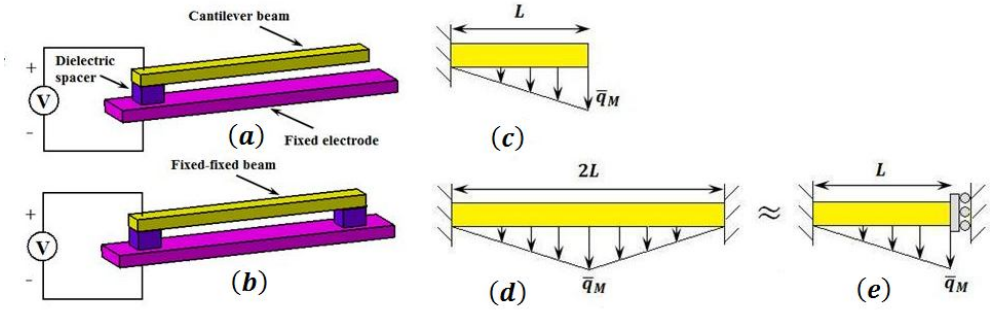

Figure 1. (a) a typical cantilever switch, (b) a typical fixed-fixed switch (c) LDL model for a cantilever nano-beam, (d) LDL model for a fixed-fixed nano-beam and (e) an equivalent fixed-fixed nano-beam.

According to the hybrid nonlocal beam model [4], the strain energy of the Euler-Bernoulli beam is expressed as a combination of local and nonlocal curvatures as follow:

$$U_e = \frac{1}{2}\int_0^L \tilde{E}I(\kappa\tilde{\kappa} + a^2\kappa'\tilde{\kappa}'), \tag{1}$$

where $\kappa = \frac{d^2y}{dx^2}$, $a = \alpha l_c$ and $(\ )'$ denotes $\frac{d}{dx}$. In Equation 1, x is the longitudinal coordinate measured from the left end of the beam, I is the second moment of cross-sectional area of the beam, y is transverse displacement, l_c is characteristic length, α is a positive dimensionless parameter which acts as a regularizing factor and $\tilde{E}$ is the effective modulus. Also, κ and $\tilde{\kappa}$ are the local and nonlocal curvatures, respectively, which are related by the following differential equation:

$$\tilde{\kappa} - l_c^2\tilde{\kappa}'' = \kappa \tag{2}$$

If q denotes transverse load per unit length of the beam, the work of potential forces, U_p, may be written as:

$$U_p = -\int_0^L qy dx, \tag{3}$$

According to the principle of stationary value of the total potential energy, for equilibrium, the first variation of the total potential, $U_t = U_p + U_e$, must be zero:

$$\delta(U_t) = 0, \tag{4}$$

Thus, the equilibrium equation and the boundary conditions are obtained from Equation 4 as:

$$M'' - q = 0, \tag{5}$$

$$\begin{gathered} M' = 0 \text{ or } y = 0 \text{ at } x = 0, L, \\ M = 0 \text{ or } y' = 0 \text{ at } x = 0, L, \\ \tilde{\kappa}' = 0 \text{ at } x = 0, L, \end{gathered} \tag{6}$$

where bending moment M is given by:

$$M = \tilde{E}I(\tilde{\kappa} - a^2\tilde{\kappa}''). \tag{7}$$

Using Equation 2 and 7, bending moment can be obtained as:

$$M = \tilde{E}I[(1-\alpha^2)\tilde{\kappa} + \alpha^2\kappa]. \tag{8}$$

Equation 8 may be written as:

$$M - l_c^2 M'' = \tilde{E}I(\kappa - a^2\kappa''). \tag{9}$$

Substituting for the second derivative of M from Equation 5 into Equation 9 gives:

$$M = \widetilde{E}I\left(-(\alpha l_c)^2 \frac{d^4y}{dx^4} + \frac{d^2y}{dx^2}\right) + l_c^2 q,\ Q = \frac{dM}{dx} = \widetilde{E}I\left(-(\alpha l_c)^2 \frac{d^5y}{dx^5} + \frac{d^3y}{dx^3}\right) + l_c^2 \frac{dq}{dx}, \tag{10}$$

where Q is the shear force. By substituting M from Equation 10 into Equation 5, equation of motion is obtained as:

$$\widetilde{E}I(\alpha l_c)^2 \frac{d^6y}{dx^6} - \widetilde{E}I \frac{d^4y}{dx^4} + q - l_c^2 \frac{d^2q}{dx^2} = 0, \tag{11}$$

3 Linear distributed load (LDL) model

The distributed force q in Equation 11 can be considered as:

$$q = F_e + F_n, \tag{12}$$

where F_e is the distributed electrostatic force due to the applied voltage V and F_n is the intermolecular force ($n = 3$ and 4 indicate the van der Waals and the Casimir forces, respectively). Considering the first order fringing field correction, the electrostatic force per unit length of the beam [5], the van der Waals force per unit length of the beam [6] and the Casimir force per unit length of the beam [7] take the following form:

$$F_e = \frac{\varepsilon_0 w V^2}{2(g-y)^2}\left(1 + 0.65\frac{(g-y)}{w}\right), F_3 = \frac{Aw}{6\pi(g-y)^3}, F_4 = \frac{\pi^2 \bar{h} c w}{240(g-y)^4}, \tag{13}$$

where $\varepsilon_0 = 8.854 \times 10^{-12} C^2 N^{-1} m^{-2}$ is the permittivity of vacuum, A is the Hamaker constant, $\bar{h} = 1.055 \times 10^{-34} J$ is Planck's constant divided by 2π and $c = 3 \times 10^8 ms^{-1}$ is the speed of light. It is convenient to express all of the parameters in non-dimensional form. To do this, the following parameters are introduced:

$$\bar{x} = \frac{x}{L}, u = \frac{y}{g}, \eta = \frac{l_c}{L}, \xi = \frac{\alpha l_c}{L}, \overline{M} = \frac{ML^2}{\widetilde{E}Ig}, \overline{Q} = \frac{QL^3}{\widetilde{E}Ig}, \tau_3 = \frac{AwL^4}{6\pi g^4 \widetilde{E}I}, \tau_4 = \frac{\pi^2 \bar{h} c w L^4}{240 g^5 \widetilde{E}I},$$
$$\gamma = \frac{\varepsilon_0 w V^2 L^4}{2g^3 \widetilde{E}I}, f = 0.65\frac{g}{w}, \overline{q} = \frac{qL^4}{\widetilde{E}Ig}. \tag{14}$$

Using the non-dimensional parameters, Equations 10, 11 and 12 become:

$$\overline{M} = -\xi^2 \frac{d^4u}{d\bar{x}^4} + \frac{d^2u}{d\bar{x}^2} + \eta^2 \overline{q},\ \overline{Q} = -\xi^2 \frac{d^5u}{d\bar{x}^5} + \frac{d^3u}{d\bar{x}^3} + \eta^2 \frac{d\overline{q}}{d\bar{x}}, \tag{15}$$

$$\xi^2 \frac{d^6u}{d\bar{x}^6} - \frac{d^4u}{d\bar{x}^4} + \overline{q} - \eta^2 \frac{d^2\overline{q}}{d\bar{x}^2} = 0, \tag{16}$$

$$\overline{q}(\bar{x}) = \frac{\tau_n}{[1-u(\bar{x})]^n} + \frac{\gamma}{[1-u(\bar{x})]^2} + f\frac{\gamma}{[1-u(\bar{x})]}. \tag{17}$$

Equations 6 in non-dimensional form become:

$$\begin{aligned} \overline{M}' = 0 \text{ or } u = 0 \text{ at } \bar{x} = 0,1, \\ \overline{M} = 0 \text{ or } \frac{du}{d\bar{x}} = 0 \text{ at } \bar{x} = 0,1, \\ \xi^2 \frac{d^5 u}{d\bar{x}^5} + (\alpha^2 - 1)\frac{d^3 u}{d\bar{x}^3} - \eta^2 \frac{d\bar{q}}{d\bar{x}} = 0 \text{ at } \bar{x} = 0,1. \end{aligned} \tag{18}$$

Due to the nonlinearity of the distributed lateral load $\bar{q}(\bar{x})$, the exact solution of Equation 16 is complicated; therefore, in order to solve this equation, the distributed lateral load is approximated by a linear function of $\bar{x}$ (LDL model) [3]. This approximation is shown in Figure 1(c) and 1(d), where $\bar{q}_M$ denotes the maximum load density at the free end and mid-point of the cantilever and fixed-fixed nano-beams, respectively. Based on the LDL model, the lateral load $\bar{q}(\bar{x})$ for both cantilever and fixed-fixed nano-beams is approximated by:

$$\bar{q} = \bar{q}_M \bar{x}. \tag{19}$$

Substitution of Equation 19 into Equation 16 leads to:

$$\xi^2 \frac{d^6 u}{d\bar{x}^6} - \frac{d^4 u}{d\bar{x}^4} = -\bar{q}_M \bar{x}. \tag{20}$$

The solution of Equation 20 may be written as:

$$u(\bar{x}) = C_1 \cosh\left(\frac{\bar{x}}{\xi}\right) + C_2 \sinh\left(\frac{\bar{x}}{\xi}\right) + \frac{\bar{q}_M}{120}\bar{x}^5 + C_3\bar{x}^3 + C_4\bar{x}^2 + C_5\bar{x} + C_6. \tag{21}$$

4 Pull-in voltages

The tip deflection of the cantilever beam and the mid-point deflection of the fixed-fixed beam may be defined as:

$$u_M = C_H \bar{q}_M,\ C_H = C_1 \cosh\left(\frac{1}{\xi}\right) + C_2 \sinh\left(\frac{1}{\xi}\right) + \frac{\bar{q}_M}{120} + C_3 + C_4 + C_5 + C_6. \tag{22}$$

From Equation 17 it is obvious that:

$$\bar{q}_M = \frac{\tau_n}{[1-u_M]^n} + \frac{\gamma}{[1-u_M]^2} + f\frac{\gamma}{[1-u_M]}. \tag{23}$$

Substitution of Equation 23 into Equation 22 and then by setting $d\gamma/du_M = 0$ to get γ_{PI} the pull-in voltage, is obtained as:

$$V_{PI} = \left(\frac{2g^3 \tilde{E} I \gamma_{PI}}{\varepsilon_0 w L^4}\right)^{\frac{1}{2}} \tag{24}$$

5 Freestanding nano-beams

When the electrode/ground separation is sufficiently small, due to the intermolecular forces, the movable electrode might collapse onto the fixed electrode without the application of external voltage. The maximum length of the electrode in which the collapse does not occur, $L_{\max}$, is denoted as the detachment length. Alternatively, for a known electrode length, a minimum electrode/ground gap, $g_{\min}$, exists that ensures the electrode does not adhere to the substrate as a result of the intermolecular forces. The detachment length and the minimum gap that are the basic design parameters in nano-switch structures can be obtained as:

$$L_{3^{\max}} = \sqrt[4]{\frac{6\pi\tau_3^* g^4 \tilde{E}I}{Aw}}, L_{4^{\max}} = \sqrt[4]{\frac{240\tau_4^* g^5 \tilde{E}I}{\pi^2 \bar{h} cw}}, g_{3^{\min}} = \sqrt[4]{\frac{AwL^4}{6\pi\tau_3^* \tilde{E}I}}, g_{4^{\min}} = \sqrt[5]{\frac{\pi^2 \bar{h} cwL^4}{240\tau_4^* \tilde{E}I}}, \quad (25)$$

where τ_3^* is the critical value for the non-dimensional form of van der Waals force and τ_4^* is the critical value for the non-dimensional form of Casimir force when $\gamma = 0$ and they can be obtained from Equation 23. $L_{3^{\max}}$, $L_{4^{\max}}$, $g_{3^{\min}}$ and $g_{4^{\min}}$ are the detachment length of the nano-beam due to the van der Waals force, the detachment length of the nano-beam due to the Casimir force, the minimum gap value due to the van der Waals force and the minimum gap value due to the Casimir force, respectively.

6 Numerical examples

It can be seen that the pull-in voltages, detachment lengths and minimum gap values depend on two length variables, namely, η and $\xi = \alpha\eta$, where α is a positive dimensionless parameter acting as a regularizing factor. In this section, numerical results are presented that examine the effects of the small length-scale parameter η and regularizing factor α on the pull-in voltages and detachment lengths. For the numerical examples, a silicon movable electrode is considered with Young's modulus $E = 176GPa$, Hamaker constant between silicon and highly oriented pyrolytic graphite (HOPG) $A = 2.96 \times 10^{-19}$, $h = 3.5$ nm and $w = 18$ nm. The gap between the two electrodes for the van der Waals and the Casimir forces are considered to be 16 nm and 25 nm, respectively.

Variations of the pull-in voltages with small-scale parameter η for different values of regularizing factor α are examined for a cantilever nano-beam with a length of 200 nm. Figures 2(a) and (b) show the variations of the pull-in voltages subjected to the van der Waals and Casimir forces, respectively. It should be noted that the results for the case $\alpha = 0$ corresponds to the nonlocal Euler-Bernoulli beam theory, while $\alpha = 1$ corresponds to the local beam theory, where small-scale effects are ignored. Figures 3(a) and (b) show variations of the pull-in voltages with small-scale parameter η for different values of regularizing factor α for a 200 nm long fixed-fixed nano-beam. From figures 2-3 it can be seen that as the small-scale parameter η increases, the pull-in voltage decreases for $\alpha \prec 1$, whereas it increases for $\alpha \succ 1$. At a certain η value, when the regularizing factor α increases, the pull-in voltage increases as well. The small-scale coefficient η and the regularizing factor α have same effects on the pull-in voltage of both the cantilever and fixed-fixed nano-beams except in the Eringen's nonlocal beam model, where for a cantilever nano-beam, an increase in the small-scale factor leads to a higher pull-in voltage, whereas for a fixed-fixed nano-beam it results in a lower pull-in voltage. In the Eringen's nonlocal theory, the internal small-length

scale enters into the constitutive equation as a material parameter; therefore, with the increase of the small length-scale parameter, the pull-in behavior of both cantilever and fixed-fixed nano-beams should be affected in the same way and the boundary conditions shouldn't affect the behavior of nano-beams differently. For this reason, a paradox can be observed in the Eringen's nonlocal model, which can be eliminated by using the hybrid nonlocal theory. In addition, in the hybrid model, the pull-in voltage behavior depends significantly on the magnitude of the regularizing factor α .

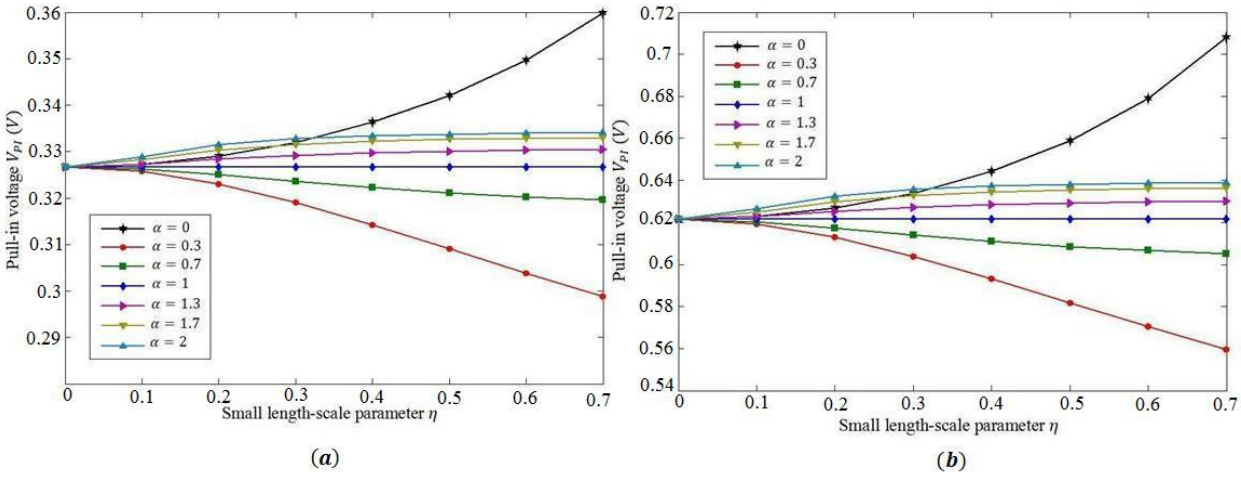

Figure 2. Variations of the pull-in voltage with small length-scale parameter η for different values of regularizing factor α for a cantilever beam subjected to (a) van der Waals force, (b) Casimir force.

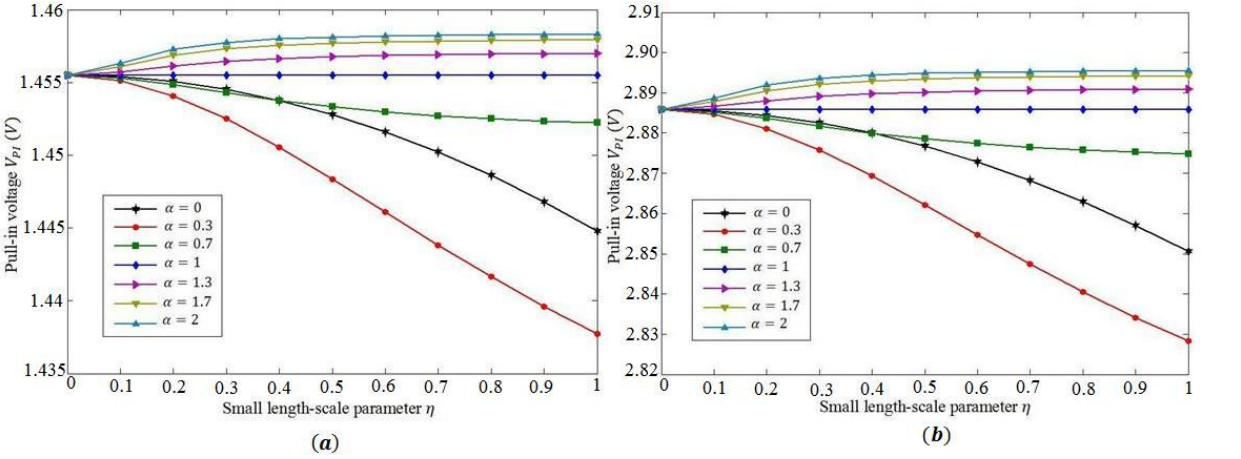

Figure 3. Variations of the pull-in voltage with small length-scale parameter η for different values of regularizing factor α for a fixed-fixed beam subjected to (a) van der Waals force, (b) Casimir force.

Variations of the maximum length of the cantilever beam with small length-scale parameter, η , for different values of the regularizing factors, α , subjected to the van der Walls and Casimir forces are respectively shown in figures 4(a) and (b). For a given small-scale parameter η , it may be observed that with increasing α the maximum length of the cantilever beam increases. Based on the hybrid nonlocal model, as the small-scale parameter η increases, the maximum length of the cantilever beam decreases for $\alpha \prec 1$, whereas it increases for $\alpha \succ 1$.

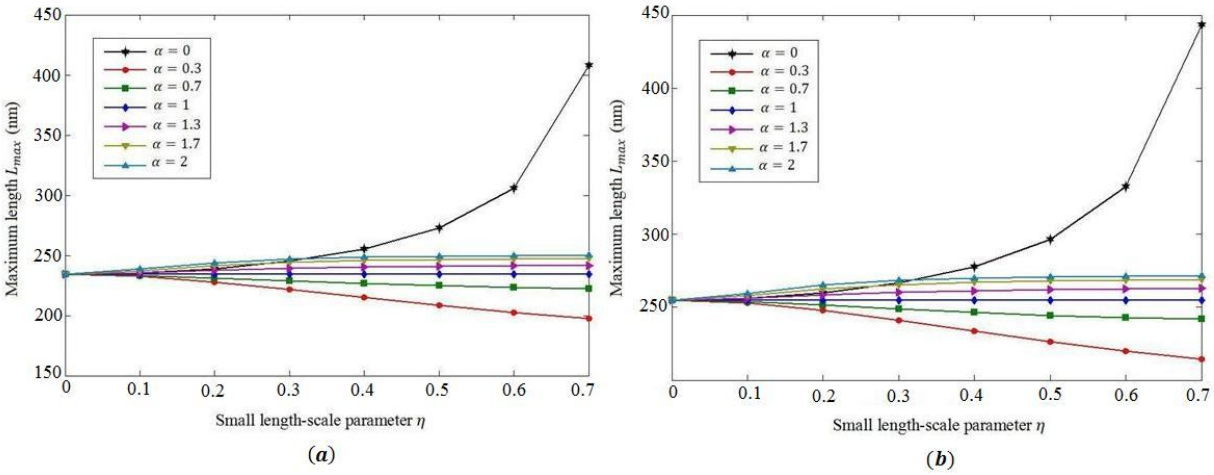

Figure 4. Variations of the maximum length, $L_{\max}$, with the small length-scale parameter η for different regularizing factor α for a cantilever beam subjected to (a) van der Waals force, (b) Casimir force.

7 Conclusion

On the basis of hybrid nonlocal Euler-Bernoulli beam model, the pull-in instability of nano-switches under intermolecular and electrostatic forces is studied. The governing equations are derived and the closed form solutions are obtained based on the LDL model. The freestanding behavior of the nano-beams is also investigated. The numerical results show that the pull-in voltages, detachment lengths and minimum gaps between the electrodes and the ground are affected significantly by both the small length-scale parameter η and the regularizing factor α. However, for the two types of the nano-electrodes considered, the Eringen's nonlocal beam model produces unreasonable results. These shortcomings of Eringen's nonlocal beam theory can be resolved by employing the hybrid nonlocal beam model. Based on the hybrid nonlocal Euler-Bernoulli beam model, for $\alpha \prec 1$, it has been shown that as the small-scale coefficient η increases, the pull-in voltages and detachment lengths decrease. The results for the case of $\alpha \succ 1$ are opposite to the results for $\alpha \prec 1$. At a certain η value, by increasing the regularizing factor α, the pull-in voltages and detachment lengths increase.

Rererrence

[1]Li G., Alura N.R. A Lagrangian approach for quantum-mechanical electrostatic analysis of deformable silicon nanostructures. *Eng. Bound. Elem*, **30**, pp. 925-932 (2006).

[2]Eringen A.C., Edelen D.G.B. On nonlocal elasticity. *Int. J. Eng. Sci*, **10**, pp. 233-248 (1972).

[3]Yang J., Jia X.L., Kitipornchai S. Pull-in instability of nano-switches using nonlocal elasticity theory. *J. Phys. D. Appl. Phys*, **41**, pp. 035103 (2008).

[4]Challamel N. Wang C.M. The small length-scale effect for a nonlocal cantilever beam: a paradox solved. *Nanotechnology*, **19** pp. 345703 (2008).

[5]Haung J.M., Liew K.M., Wong C.H., Rajendran S., Tan M.J. and Liu A.Q. Mechanical design and optimization of capacitive micro machined switch. *Sensor. Actuat. A-phys*, **1993**, pp. 273-285 (2001).

[6]Israelachvili J.N. *Intermolecular and Surface Forces.* Academic Press, London (1992).

[7]Lamoreaux S.K. The Casimir force: background, experiments, and applications. *Rep. Prog. Phys*, **68** pp. 201-236(2005).